Reduced purities as measures of decoherence in many-electron systems

Ignacio Franco and Heiko Appel

Reduced purities as measures of decoherence in many-electron systems

Ignacio Franco[a)] and Heiko Appel
Theory Department, Fritz Haber Institute of the Max Planck Society, Faradayweg 4-6, 14195 Berlin, Germany

A hierarchy of measures of decoherence for many-electron systems that is based on the purity and the hierarchy of reduced electronic density matrices is presented. These reduced purities can be used to characterize electronic decoherence in the common case when the many-body electronic density matrix is not known and only reduced information about the electronic subsystem is available. Being defined from reduced electronic quantities, the interpretation of the reduced purities is more intricate than the usual (many-body) purity. This is because the nonidempotency of the r-body reduced electronic density matrix that is the basis of the reduced purity measures can arise due to decoherence or due to electronic correlations. To guide the interpretation, explicit expressions are provided for the one-body and two-body reduced purities for a general electronic state. Using them, the information content and structure of the one-body and two-body reduced purities is established, and limits on the changes that decoherence can induce are elucidated. The practical use of the reduced purities to understand decoherence dynamics in many-electron systems is exemplified through an analysis of the electronic decoherence dynamics in a model molecular system. © *2013 AIP Publishing LLC.*
[http://dx.doi.org/10.1063/1.4819819]

I. INTRODUCTION

An ubiquitous process in nature is that of decoherence,[1–4] which refers to the decay of quantum correlations of a quantum subsystem because of interaction with an environment. Understanding decoherence is central to our description of basic processes such as measurement, photosynthesis, vision, or electron transfer,[5–13] to the development of approximation schemes that describe the system-bath dynamics[1, 14–21] and it is the starting point for the design of methods to preserve coherence in materials that can be subsequently exploited in intriguing and potentially useful ways via quantum control[22, 23] or quantum information[24] schemes.

Here, we introduce measures of decoherence that can be used for the description of the coherence properties of many-electron systems in the presence of an environment. The proposed measures are generalizations of the purity that employ the few-body electronic reduced density matrices instead of the full many-body reduced density matrix, and are thus more readily available for the characterization of coherence in many-body systems. However, because these measures are based on reduced electronic quantities, their interpretation differs in key aspects and can be more intricate from the one of the usual N-body purity. Below we discuss the properties, merits, and limitations of the reduced purity measures.

The structure of this paper is as follows. In Sec. II, we briefly review basic decoherence ideas as they apply to many-electron systems. Then, in Sec. III, we introduce a hierarchy of reduced purity measures that are based on the well-known hierarchy[25, 26] of reduced electronic density matrices. In particular, we determine analytical expressions for the reduced

purities that follow from the one- and two-body reduced density matrices for a general time-dependent correlated electronic state (Secs. III A–III C). Using these expressions, we then discuss in Sec. III D the interpretation of the reduced purities and the effect of electronic correlation on their evolution. Finally, in Sec. IV we exemplify the use of the reduced purities by studying electronic decoherence in a vibronic system. We summarize our main findings in Sec. V.

II. PURITY AND THE INTERPRETATION OF DECOHERENCE

Consider a N-particle electronic system interacting with an environmental bath, with system-bath Hamiltonian of the form $H = H_e + H_B + H_{e-B}$, where H_e is the electronic Hamiltonian, H_B the bath Hamiltonian, and H_{e-B} is the system-bath coupling. In light of the Schmidt decomposition,[24] a pure state of the bipartite system can always be written as an entangled state of the form

$$|\Omega(t)\rangle = \sum_n \sqrt{\lambda_n}|\Psi_n\rangle|B_n\rangle, \tag{1}$$

where $|\Psi_n\rangle$ are orthonormal states of the electronic subsystem and $|B_n\rangle$ orthonormal states of the bath. The Schmidt coefficients $\sqrt{\lambda_n}$ are nonnegative real numbers satisfying $\sum_n \lambda_n = 1$. It is often useful to express Eq. (1) in terms of the N-particle eigenbasis $|E_n\rangle$ of the many-electron Hamiltonian H_e. Since the $\{|E_n\rangle\}$ form a complete set in the subsystem Hilbert space, in general $|\Psi_n\rangle = \sum_m c_{mn}|E_m\rangle$. Thus, Eq. (1) can be rewritten as

$$|\Omega(t)\rangle = \sum_n |E_n\rangle|\chi_n(t)\rangle, \tag{2}$$

a)Present address: Department of Chemistry, University of Rochester, Rochester, New York 14627, USA. Electronic mail: franco@chem.rochester.edu

where the bath states associated with each of the $|E_n\rangle$ are defined by $|\chi_n\rangle = \sum_m c_{nm}\sqrt{\lambda_n}|B_m\rangle$. The $\{|\chi_n\rangle\}$ are not orthonormal but do satisfy $\sum_n \langle \chi_n|\chi_n\rangle = 1$.

The properties of the electronic subsystem for such an entangled state $|\Omega\rangle$ are completely characterized by the N-particle electronic density matrix

$$\hat{\rho}_e(t) = \mathrm{Tr}_B\{|\Omega\rangle\langle\Omega|\} = \sum_{nm} \langle\chi_m(t)|\chi_n(t)\rangle|E_n\rangle\langle E_m|, \quad (3)$$

where the trace is over the environmental degrees of freedom. Note that the coherences or phase relationship between electronic eigenstates (the off-diagonal elements) in $\hat{\rho}_e$ are determined by the overlaps $S_{nm}(t) = \langle\chi_m|\chi_n\rangle$ between the environmental states associated with the electronic eigenstates. Thus, the loss of coherences in $\hat{\rho}_e(t)$ can be interpreted as the result of the decay of the S_{nm} during the coupled electron-bath evolution.[27–30] Standard measures of decoherence precisely capture this. For example, the purity, the measure of decoherence that we focus on here, is given by

$$P(t) = \mathrm{Tr}\{\hat{\rho}_e^2(t)\} = \sum_{nm} |\langle\chi_m(t)|\chi_n(t)\rangle|^2 = \sum_n \lambda_n(t)^2 \quad (4)$$

and decays with the overlaps between the environmental states S_{nm}.

III. A HIERARCHY OF REDUCED MEASURES OF ELECTRONIC DECOHERENCE

In order to quantify the coherence of a given many-particle electron system, one ideally would like to study the N-body purity in Eq. (4) directly. It is simple to interpret ($P = 1$ for pure states; $P < 1$ for mixed states; $P = 1/M$ for a maximally entangled M-level subsystem), it has well-defined upper and lower values and captures all possible electronic coherences. This, however, is not always possible because of the many-body nature of the problem. To determine the purity from a time-dependent simulation, one has to either propagate the many-body electronic density matrix [Eq. (3)] or follow the dynamics of the bath. Either approach is intractable in general except for few-level problems because of the inherent difficulty in solving the many-body problem (see, e.g., Ref. 31) and/or because of the high-dimensionality of the objects involved. A reduced method to capture the essential electronic coherences is thus desirable.

Here, we introduce a hierarchy of measures of coherence in many-particle systems that is based on the well-known hierarchy of many-particle reduced density matrices.[25, 26] Specifically, we define the r-body reduced purity (or r-body purity, for short) as

$$P_r(t) = \mathrm{Tr}\{^{(r)}\hat{\Gamma}(t)^2\} = \sum_n {}^{(r)}\lambda_n^2, \quad (5)$$

where $^{(r)}\hat{\Gamma}$ refers to the r-body reduced electronic density matrix and the set $\{^{(r)}\lambda_n\}$ to its eigenvalues. The matrix elements of $^{(r)}\hat{\Gamma}$ can be expressed as

$$^{(r)}\Gamma_{i_1 i_2 \dots i_r}^{j_1 j_2 \dots j_r}(t) = \frac{1}{r!}\mathrm{Tr}\{\hat{c}_{i_1}^\dagger \hat{c}_{i_2}^\dagger \dots \hat{c}_{i_r}^\dagger \hat{c}_{j_r} \dots \hat{c}_{j_2} \hat{c}_{j_1} \hat{\rho}_e(t)\}. \quad (6)$$

Here, the operator $\hat{c}_i^\dagger$ (or $\hat{c}_i$) creates (or annihilates) a fermion in the ith spin-orbital of the basis set and satisfies the usual fermionic anticommutation rules ($\{\hat{c}_i, \hat{c}_j^\dagger\} = \delta_{i,j}$, $\{\hat{c}_i^\dagger, \hat{c}_j^\dagger\} = \{\hat{c}_i, \hat{c}_j\} = 0$). Note that from the r-body reduced density matrix one can obtain all other lower-order ($r - s$) density matrices by contractions of the indices, and thus all lower-order purities. In general,

$$\sum_{i_p} {}^{(r+1)}\Gamma_{i_1 \dots i_p \dots i_{r+1}}^{j_1 \dots j_p \dots j_{r+1}}(t) = \frac{N-r}{r+1} {}^{(r)}\Gamma_{i_1 i_2 \dots i_r}^{j_1 j_2 \dots j_r}(t), \quad (7)$$

where p is an integer between 1 and $r + 1$. The fully contracted r-body density matrix yields

$$\sum_{i_1,\dots,i_r} {}^{(r)}\Gamma_{i_1 \dots i_r}^{i_1 \dots i_r}(t) = \frac{N!}{r!(N-r)!}. \quad (8)$$

Using this notation, the r-body purity can be expressed as

$$P_r(t) = \sum_{\substack{i_1,\dots,i_r \\ j_1,\dots,j_r}} {}^{(r)}\Gamma_{i_1,\dots,i_r}^{j_1,\dots,j_r}(t) {}^{(r)}\Gamma_{j_1,\dots,j_r}^{i_1,\dots,i_r}(t). \quad (9)$$

Note that, because the trace is independent of the basis, the expression above is valid in any complete single-particle basis-set. Further note that it is also possible to define the r-body purity based on the spin-contracted r-body electronic density matrix.[32] However, the structure of the spin-uncontracted version adopted here is simpler and more amenable to generalization.

Because the r-body purity in Eq. (5) is defined by the reduced density matrix $^{(r)}\hat{\Gamma}$ obtained by tracing over the bath *and* $N - r$ electronic coordinates, it can be argued that the P_r are a measure of decoherence due to interactions with the bath *and* the traced out electronic degrees of freedom. However, since electrons are indistinguishable there is no operator that can take advantage of electronic entanglements or distinguish between an electronic "subsystem" and an electronic "bath". Thus, we view the reduced purities as measures of the coherence of many-electron systems that can be used in the usual case when only partial information about the electronic system is known. Nevertheless, because of their reduced nature, their interpretation requires more care and differs in a few key aspects from the N-body purity in Eq. (4) in ways that are discussed in detail below.

A. Using Slater determinants to define a coherence order

We are concerned with the coherence properties of a general N-particle correlated time-dependent electronic density matrix $\hat{\rho}_e$ [Eq. (3)]. Without loss of generality, it is convenient to express $\hat{\rho}_e$ in terms of Slater determinants as

$$\hat{\rho}_e = \sum_{n,m} a_{nm}|\Phi_n\rangle\langle\Phi_m|, \quad (10)$$

where $|\Phi_n\rangle$ corresponds to a single Slater determinant with integer occupation numbers in a given (arbitrary) single-particle basis $|\epsilon\rangle = \hat{c}_\epsilon^\dagger|0\rangle$, where $|0\rangle$ is the vacuum level. In writing Eq. (10), we have expanded the correlated electronic states in Eq. (3) in terms of a basis of Slater determinants, i.e., in

a full configuration interaction expansion $|E_i\rangle = \sum_n b_{ni}|\Phi_n\rangle$. The a_{nn} in Eq. (10) denote the population of Slater determinant n, while the a_{nm} refer to the coherences between the n, m pair. In this context, we define the *order s_{nm} of a given pair of Slater determinants* $|\Phi_n\rangle$ *and* $|\Phi_m\rangle$ as the number of single particle transitions required to do a $|\Phi_n\rangle \rightarrow |\Phi_m\rangle$ transition. This quantity can be computed by

$$s_{nm} = N - \sum_\epsilon f_n(\epsilon) f_m(\epsilon), \qquad (11)$$

where $f_n(\epsilon)$ is the distribution function of the single-particle levels ϵ in state $|\Phi_n\rangle$. The quantity $f_n(\epsilon)$ is defined by

$$\langle \Phi_n | \hat{c}_\epsilon^\dagger \hat{c}_{\epsilon'} | \Phi_n \rangle = f_n(\epsilon) \delta_{\epsilon,\epsilon'}, \qquad (12)$$

and takes values of 0 or 1 depending on whether the orbital level ϵ is occupied or not. The quantity $s_{nm} \in [0, N]$ and takes the value 1 for pairs of states that differ by single excitations, 2 for doubles, etc. *We will refer to a coherence between states* $|\Phi_n\rangle$ *and* $|\Phi_m\rangle$ *as a coherence of order s_{nm}.*

We now use these definitions to discuss properties of the reduced purities.

B. The *r*-body purity can only distinguish coherences of order *r* or less

First note that, *because the r-body purity is constructed from the r-body density matrix, it is only informative about electronic coherences of order $s \leq r$.* That is, it cannot distinguish between a superposition and a mixed state between Slater determinants that differ by $r + 1$ (or more) particle transitions. This is in contrast with the N-body purity where all possible coherences in the system are evident.

To make this observation evident, consider the r-body density matrix associated with the general N-particle density matrix in Eq. (10),

$$^{(r)}\Gamma_{i_1 i_2 \dots i_r}^{j_1 j_2 \dots j_r} = \frac{1}{r!} \sum_{n,m} a_{nm} \langle \Phi_m | \hat{c}_{i_1}^\dagger \hat{c}_{i_2}^\dagger \dots \hat{c}_{i_r}^\dagger \hat{c}_{j_r} \dots \hat{c}_{j_2} \hat{c}_{j_1} | \Phi_n \rangle. \qquad (13)$$

The coherences between states n and m in the N-particle density matrix can only contribute to the r-body reduced density matrix if $\langle \Phi_m | \hat{c}_{i_1}^\dagger \hat{c}_{i_2}^\dagger \dots \hat{c}_{i_r}^\dagger \hat{c}_{j_r} \dots \hat{c}_{j_2} \hat{c}_{j_1} | \Phi_n \rangle \neq 0$. For this to happen, there has to be some r-body transition that connects the two states. Hence, if the two states differ by $s > r$ particle transitions any coherences that may exist between them is simply not reflected in the r-body density matrix and hence in the r-body purity.

C. A closer look into the one-body and two-body purities

To isolate additional properties of the reduced purities and to illustrate their interpretation, we now determine explicit expressions for P_1 and P_2 for the general electronic density matrix in Eq. (10). While it is possible to calculate higher order reduced purities through judicious application of Wick's theorem,[31,33] the one-body and two-body purities are the most important and readily applicable cases. To proceed, it is useful to first determine the purity for the simpler case

where the density matrix only involves two N-particle Slater determinants

$$\hat{\rho}_e = \sum_{n,m=1}^{2} a_{nm} |\Phi_n\rangle \langle \Phi_m| \qquad (14)$$

and then extend the solution to an arbitrary number of $|\Phi_n\rangle$ states. Without loss of generality, we suppose that $|\Phi_2\rangle$ is at most two-particle transitions away from $|\Phi_1\rangle$ since only coherences of order 2 or less are visible in P_2. We choose $|\Phi_1\rangle$ as the reference state and write

$$|\Phi_2\rangle = \hat{c}_{\alpha_2}^\dagger \hat{c}_{\beta_2} \hat{c}_{\alpha_1}^\dagger \hat{c}_{\beta_1} |\Phi_1\rangle. \qquad (15)$$

In order to guarantee that $|\Phi_1\rangle \neq |\Phi_2\rangle$, we choose $\alpha_1 \neq \beta_1$ and $\alpha_2 \neq \beta_2$. Since we are interested in $|\Phi_2\rangle \neq 0$, then $\beta_1 \neq \beta_2$, $\alpha_1 \neq \alpha_2$, and $\hat{c}_{\beta_1}^\dagger |\Phi_1\rangle = \hat{c}_{\alpha_1}|\Phi_1\rangle = \hat{c}_{\alpha_2}|\Phi_1\rangle = 0$. The particular case where $|\Phi_2\rangle$ and $|\Phi_1\rangle$ differ by a single-particle transition is obtained when $\beta_2 = \alpha_1$.

From Eq. (9), P_1 is given by

$$P_1 = \sum_{\epsilon_1, \epsilon_2} {}^{(1)}\Gamma_{\epsilon_1}^{\epsilon_2}{}^{(1)}\Gamma_{\epsilon_2}^{\epsilon_1}, \qquad (16)$$

where, for convenience, the trace has been expressed in the ϵ-basis where Eq. (12) holds. In this basis, the one-body reduced density matrix for the model state in Eq. (14) is given by

$$\begin{aligned}
{}^{(1)}\Gamma_{\epsilon_1}^{\epsilon_2} &= \delta_{\epsilon_1,\epsilon_2} \left[a_{11} f_1(\epsilon_1) + a_{22} f_2(\epsilon_1) \right] \\
&\quad + \delta_{\alpha_1,\beta_2} f_1(\beta_1)(1 - f_1(\alpha_1))(1 - f_1(\alpha_2)) \\
&\quad \times [a_{12}\delta_{\epsilon_1,\alpha_2}\delta_{\epsilon_2,\beta_1} + a_{12}^\star \delta_{\epsilon_1,\beta_1}\delta_{\epsilon_2,\alpha_2}], \qquad (17)
\end{aligned}$$

where we have taken Eqs. (12) and (15) into account and used the fermionic anticommutation relations. Inserting Eq. (17) into (16) yields

$$\begin{aligned}
P_1 = \sum_\epsilon (a_{11} f_1(\epsilon) + a_{22} f_2(\epsilon))^2 \\
+ 2|a_{12}|^2 f_1(\beta_1)(1 - f_1(\alpha_1))(1 - f_1(\alpha_2))\delta_{\alpha_1,\beta_2}.
\end{aligned}$$

Now, supposing that $|\Phi_2\rangle \neq 0$ (such that $f_1(\beta_1)(1 - f_1(\alpha_1))(1 - f_1(\alpha_2)) = 1$) and noting that the requirement that $\alpha_1 = \beta_2$ is equivalent to requiring $s_{12} = 1$, then

$$P_1 = \sum_\epsilon (a_{11} f_1(\epsilon) + a_{22} f_2(\epsilon))^2 + 2|a_{12}|^2 \delta_{s_{12},1}, \qquad (18)$$

which determines the one-body purity for the two-state system in Eq. (14).

Extending the previous discussion to the general case, the one-body purity for a many-body state of the form in Eq. (10) is given by

$$\begin{aligned}
P_1 &= \sum_\epsilon \left(\sum_n a_{nn} f_n(\epsilon) \right)^2 + 2 \sum_{n>m} |a_{nm}|^2 \delta_{s_{nm},1} \\
&= N - 2 \sum_{n>m} (a_{nn} a_{mm} s_{nm} - |a_{nm}|^2 \delta_{s_{nm},1}), \qquad (19)
\end{aligned}$$

where the first two terms in the second line depend on the populations in the expansion of $\hat{\rho}_e$ in Eq. (10), while the last one characterizes the contributions due to the coherences. In writing Eq. (19), we have extended the process that lead to Eq. (18) to accommodate an arbitrary number of states and

taken into account Eq. (11), the state normalization $\sum_n a_{nn} = 1$, and the fact that $\sum_\epsilon f_n(\epsilon) = N$. Note that, as pointed out previously, $P_1(t)$ decreases with the decoherence between states that differ by one-particle transitions and is unaffected by decoherence processes that involve higher-order coherences.

The derivation of P_2 proceeds along similar lines. In the ϵ-basis, P_2 can be expressed as

$$P_2 = \sum_{\epsilon_1,\epsilon_2,\epsilon_3,\epsilon_4} {}^{(2)}\Gamma_{\epsilon_1,\epsilon_2}^{\epsilon_4,\epsilon_3} {}^{(2)}\Gamma_{\epsilon_4,\epsilon_3}^{\epsilon_1,\epsilon_2}. \tag{20}$$

Here, the matrix elements determining ${}^{(2)}\Gamma_{\epsilon_1,\epsilon_2}^{\epsilon_4,\epsilon_3}$ and P_2 for the two-state model in Eq. (14) are given by

$$\langle\Phi_n|\hat{A}|\Phi_n\rangle = f_n(\epsilon_3)f_n(\epsilon_4)(\delta_{\epsilon_1,\epsilon_4}\delta_{\epsilon_2,\epsilon_3} - \delta_{\epsilon_1,\epsilon_3}\delta_{\epsilon_2,\epsilon_4}),$$

$$\langle\Phi_1|\hat{A}|\Phi_2\rangle = f_1(\epsilon_1)f_1(\epsilon_2)f_1(\beta_1)(1 - f_1(\alpha_1))(1 - f_1(\alpha_2))$$
$$[\delta_{\alpha_1,\beta_2}(\delta_{\epsilon_1,\beta_1}(\delta_{\epsilon_2,\epsilon_3}\delta_{\epsilon_4,\alpha_2} - \delta_{\epsilon_2,\epsilon_4}\delta_{\epsilon_3,\alpha_2})$$
$$-\delta_{\epsilon_2,\beta_1}(\delta_{\epsilon_1,\epsilon_3}\delta_{\epsilon_4,\alpha_2} - \delta_{\epsilon_1,\epsilon_4}\delta_{\epsilon_3,\alpha_2}))$$
$$+(\delta_{\epsilon_2,\beta_1}\delta_{\epsilon_1,\beta_2} - \delta_{\epsilon_2,\beta_2}\delta_{\epsilon_1,\beta_1})$$
$$\times(\delta_{\epsilon_4,\alpha_2}\delta_{\epsilon_3,\alpha_1} - \delta_{\epsilon_4,\alpha_1}\delta_{\epsilon_3,\alpha_2})],$$

$$\langle\Phi_2|\hat{A}|\Phi_1\rangle = f_1(\epsilon_3)f_1(\epsilon_4)f_1(\beta_1)(1 - f_1(\alpha_1))(1 - f_1(\alpha_2))$$
$$[\delta_{\alpha_1,\beta_2}(\delta_{\epsilon_4,\beta_1}(\delta_{\epsilon_2,\epsilon_3}\delta_{\epsilon_1,\alpha_2} - \delta_{\epsilon_1,\epsilon_3}\delta_{\epsilon_2,\alpha_2})$$
$$-\delta_{\epsilon_3,\beta_1}(\delta_{\epsilon_2,\epsilon_4}\delta_{\epsilon_1,\alpha_2} - \delta_{\epsilon_1,\epsilon_4}\delta_{\epsilon_2,\alpha_2}))$$
$$+(\delta_{\epsilon_3,\beta_1}\delta_{\epsilon_4,\beta_2} - \delta_{\epsilon_3,\beta_2}\delta_{\epsilon_4,\beta_1})$$
$$\times(\delta_{\epsilon_1,\alpha_2}\delta_{\epsilon_2,\alpha_1} - \delta_{\epsilon_1,\alpha_1}\delta_{\epsilon_2,\alpha_2})],$$

where $\hat{A} \equiv \hat{c}_{\epsilon_1}^\dagger \hat{c}_{\epsilon_2}^\dagger \hat{c}_{\epsilon_3} \hat{c}_{\epsilon_4}$. Using these matrix elements, it follows that

$$P_2 = \frac{1}{4} \sum_{\epsilon_1,\epsilon_2,\epsilon_3,\epsilon_4} \text{Tr}\{\hat{A}\hat{\rho}_e\}\text{Tr}\{\hat{A}^\dagger \hat{\rho}_e\}$$

$$= \frac{1}{4} \sum_{\epsilon_1,\epsilon_2,\epsilon_3,\epsilon_4} \left[\sum_{n,m=1}^{2} a_{nn}a_{mm}\langle\Phi_n|\hat{A}|\Phi_n\rangle\langle\Phi_m|\hat{A}^\dagger|\Phi_m\rangle \right.$$
$$+|a_{12}|^2(\langle\Phi_1|\hat{A}|\Phi_2\rangle\langle\Phi_2|\hat{A}^\dagger|\Phi_1\rangle$$
$$\left. +\langle\Phi_2|\hat{A}|\Phi_1\rangle\langle\Phi_1|\hat{A}^\dagger|\Phi_2\rangle) \right],$$

where all other terms in the product are zero. Calculating explicitly each of the remaining terms, the two-body reduced purity for the model density matrix is given by

$$P_2 = \sum_{n,m=1}^{2} \frac{a_{nn}a_{mm}}{2} \left[\left(\sum_\epsilon f_n(\epsilon)f_m(\epsilon)\right)^2 - \sum_\epsilon f_n(\epsilon)f_m(\epsilon) \right]$$
$$+2|a_{12}|^2 f_1(\beta_1)(1 - f_1(\alpha_1))(1 - f_1(\alpha_2))$$
$$\times[\delta_{\alpha_1,\beta_2}(N - 1) + f_1(\beta_2)].$$

This expression can be cast into a form that is simpler to generalize by taking into account that if $|\Phi_2\rangle \neq 0$, $f_1(\beta_1)(1 - f_1(\alpha_1))(1 - f_1(\alpha_2)) = 1$; and that when $\alpha_1 = \beta_2$ (or $f_1(\beta_2)$

$= 1$) the order of the coherence is $s_{12} = 1$ (or $s_{12} = 2$). Thus,

$$P_2 = \sum_{n,m=1}^{2} \frac{a_{nn}a_{mm}}{2} \left[\left(\sum_\epsilon f_n(\epsilon)f_m(\epsilon)\right)^2 - \sum_\epsilon f_n(\epsilon)f_m(\epsilon) \right]$$
$$+2|a_{12}|^2[\delta_{s_{12},1}(N - 1) + \delta_{s_{12},2}].$$

This expression can be extended to capture the behavior of the general many-body state in Eq. (10) by taking into account the contribution of all possible pairs of states. In this case,

$$P_2 = \sum_{n,m} \frac{a_{nn}a_{mm}}{2} \left[\left(\sum_\epsilon f_n(\epsilon)f_m(\epsilon)\right)^2 - \sum_\epsilon f_n(\epsilon)f_m(\epsilon) \right]$$
$$+2\sum_{n>m} |a_{nm}|^2[\delta_{s_{nm},1}(N - 1) + \delta_{s_{nm},2}]$$
$$= \frac{N(N - 1)}{2} - \sum_{n>m} a_{nn}a_{mm}s_{nm}(2N - s_{nm} - 1)$$
$$+\sum_{n>m} 2|a_{nm}|^2(\delta_{s_{nm},1}(N - 1) + \delta_{s_{nm},2}), \tag{21}$$

where we have used Eq. (11) and the fact that $\sum_n f_n(\epsilon) = N$. The first two terms are due to the populations, while the last term is due to the coherences among the Slater determinants. Note that P_2 decays with the loss of coherences of order 1 and 2.

Equations (19) and (21) exemplify the behavior of the one-body and two-body purities for a general electronic state. In deriving these equations, we have taken advantage of the structure of Slater determinants. Note, however, that the value of the reduced purities is representation-independent and does not change if a different complete single-particle basis $\{|\epsilon\rangle\}$ is employed or if no decomposition into Slater determinants is invoked. This is evidenced by Eq. (5) that shows the relationship between the reduced purities and the eigenvalues of the reduced density matrices ${}^{(r)}\lambda_n$; the ${}^{(r)}\lambda_n$ are representation independent and hence the reduced purities are also representation independent. This allows for the interpretation of the decoherence in a particular basis without loss of generality.

We now discuss a few observations that follow from these general expressions.

D. Electronic correlation and the interpretation of the reduced purities

The reduced purities offer a window into the coherence behavior of many-electron systems and allow isolating coherence effects of a particular order. Nevertheless, because the P_r are defined from reduced electronic quantities, their interpretation can be more challenging than the one of the N-body purity. Note, in particular, that while the value of the N-body purity for a pure state is always 1, the value of P_r for pure electronic states depends on the degree of electronic correlation. Electronic correlation leads to nonidempotency in the reduced density matrices (see, e.g., Refs. 34 and 35) and thus to a reduction in the reduced purity that is not due to bath-induced decoherence. As a consequence, an observed decay in the reduced purity can be due to a decay in the coherence

properties of the system, or due to a change in the correlations of the many-electron system even in the absence of decoherence.

Note that it is technically possible to construct electronic decoherence measures based on the reduced purities that solely reflect decoherence processes. To see this, it is useful to recall the Carlson-Keller theorem[36] which states that for pure bound states the nonzero eigenvalues of $^{(r)}\hat{\Gamma}$ and $^{(N-r)}\hat{\Gamma}$ are identical. Since the reduced purities are determined by such eigenvalues [recall Eq. (5)], then a quantity like $P_{N-r} - P_r$ would be identically zero for pure states and nonzero for mixed states, irrespective of the details of the system-bath evolution. While of formal interest, such measures of electronic decoherence are of little practical use because they require knowledge of high-order density matrices that are generally not available.

To understand further the structure and the information that can be gleaned from the reduced purities, consider now the limiting behavior of P_1 and P_2. For reference in the discussion, we have tabulated the main limiting values of P_1 and P_2 in Figure 1. From Eq. (19), the maximum value for P_1 is N, obtained when only a single Slater determinant is involved or when all terms in the superposition are such that $s_{nm} = 1$ and $|a_{nm}|^2 = a_{nn}a_{mm}$. In the absence of population changes, a decay in P_1 follows the decay of one-body coherences; the decoherence between states n and m with $s_{nm} = 1$ can induce a maximum decay of $2|a_{nm}|^2$. Given a set of populations $\{a_{nn}\}$, the minimum value that P_1 can achieve solely due to decoherence is $P_1 = N - 1 + \sum_n a_{nn}^2$, obtained when $s_{nm} = 1$ and $a_{nm} = 0$ for all pairs of states. Thus, the maximum possible decay in the one-body reduced purity due to decoherence is $\Delta_1 = 1 - 1/M$ and occurs when all M Slater determinants are equally populated and maximally entangled with the bath. As a consequence of this, a decay of the one-body purity beyond Δ_1 cannot be explained solely on the basis of decoherence of first order and is indicative of the involvement of states with s_{nm}'s of higher order. In fact, the absolute minimum of P_1 occurs when the density matrix is composed of equally populated states $a_{nn} = 1/M$ that all differ by N-particle transitions among each other (i.e., $s_{nm} = N, \forall n \neq m$). In this case, $P_1 = N/M$ irrespective of whether the state is a superposition state or an incoherent mixture.

The limiting cases for P_2 are shown in the lower panel of Fig. 1. The maximum value of the two-body purity [Eq. (21)] is $P_2 = N(N - 1)/2$ obtained for a single Slater determinant or for a coherent superposition where $s_{nm} = 1, \forall n \neq m$. In turn, the minimum value of $P_2 = N(N - 1)/(2M)$ is obtained when all M participating Slater determinants are equally populated ($a_{nn} = 1/M$) and differ by N-particle transitions (i.e., $s_{nm} = N$), irrespective of whether the N-body density matrix represents a pure state or not. In the absence of changes in the a_{nn}'s, a decay in P_2 signals coherence loss of order 1 or 2. Importantly, note that the magnitude of the decay actually depends on the order of the coherence that is lost; the lowest order coherences having the highest impact on the reduced purity. Specifically, the decoherence of a superposition of states differing by single-particle transitions leads to a decay of P_2 from $P_2 = N(N - 1)/2$ to $P_2 = N(N - 1)/2 - (N - 1)(1 - \sum_n a_{nn}^2)$, for a maximum decay of Δ_1
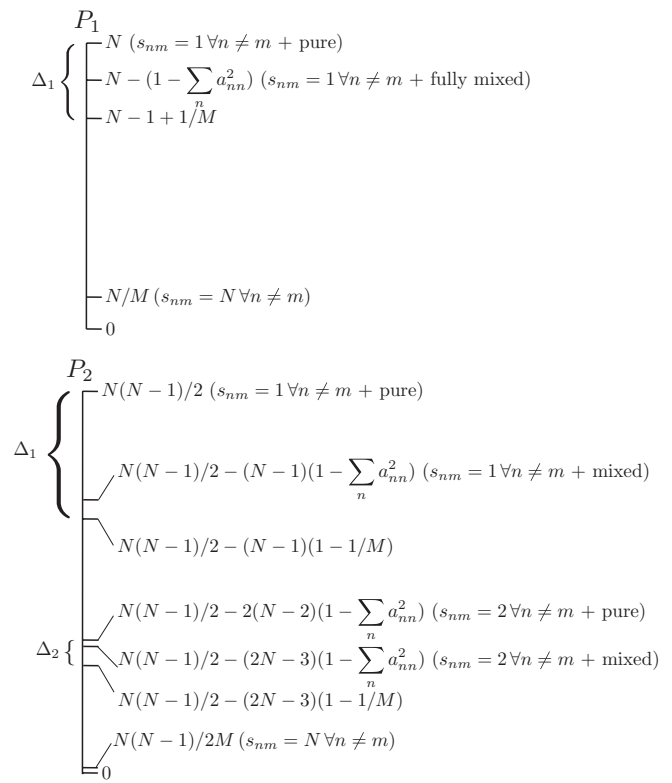

FIG. 1. Limiting values for the one-body P_1 [Eq. (19)] and two-body P_2 [Eq. (21)] purities (see text). The quantities Δ_1 and Δ_2 are the maximum possible decay of the reduced purities due to one-body and two-body decoherence, N refers to the number of electrons and M to the number of Slater determinants involved. The figure is not to scale.

$= (N - 1)(1 - 1/M)$. In turn, the decoherence of a superposition of states that differ by two-particle transitions leads to a reduction from $P_2 = N(N - 1)/2 - 2(N - 2)(1 - \sum_n a_{nn}^2)$ to $P_2 = N(N - 1)/2 - (2N - 3)(1 - \sum_n a_{nn}^2)$, for a maximum decay of $\Delta_2 = (1 - 1/M)$ which is $(N - 1)$ times less than the reduction Δ_1 due to decoherence between states for which $s_{nm} = 1$. A value of P_2 lower than $P_2 = N(N - 1)/2 - (2N - 3)$ necessarily indicates that there are $s_{nm} > 2$ in the states involved.

As seen in Eqs. (19) and (21), the decay of the reduced purities directly signals coherence loss in "pure dephasing" cases where the system-bath evolution does not lead to appreciable changes in the populations of the Slater determinants involved. More generally, the populations of the Slater determinants can change in time due to interactions of the electrons with themselves, with bath degrees of freedom or with an external potential (i.e., a laser). In such a general case, in order to cleanly identify the decoherence contributions to the dynamics of the reduced purities it is required to know the populations and the distribution functions of the Slater determinants involved. This feature is the main limiting factor in the utility of the reduced purities in characterizing decoherence effects for, generally, from a reduced density matrix it is not always easy to uniquely unravel the populations of the underlying possible Slater determinants used to describe the correlated electronic states.

However, if additional details of the problem are known, like the active determinant space and the initial state, it

then becomes increasingly plausible to perform a detailed analysis of the reduced purities on the basis of Eqs. (19) and (21) even in situations when the populations of the Slater determinants are continuously changing. We now briefly sketch how the coherence properties can be characterized: 1. Specify an active determinant space that is adequate for the problem and identify all possible determinant combinations within this space that are consistent with the orbital populations. Clearly, a very large active determinant space may make the search intractable, while a too restrictive active space may not lead to a correct characterization. 2. Fit, in each of those cases, the a_{nn}'s to reproduce the observed orbital population dynamics. If the procedure is not unique, keep track of competing possibilities. 3. Given each individual set of model $\{a_{nn}\}$, using Eq. (19) calculate two limits for the one body purity; a fully incoherent limit $P_1^{(inc)}$ where the $a_{nm} = 0$ for $n \neq m$ and a coherent limit $P_1^{(coh)}$ where $a_{nn}a_{mm} = |a_{nm}|^2$. 4. Use the observed P_1 to discard possibilities. If $P_1^{(inc)} > P_1$ or $P_1^{(coh)} < P_1$ discard the possibility, as the model state cannot possibly describe the system. 5. If the coherence properties of the initial state are known, further discard options by demanding the model to exactly reproduce $P_1(0)$. 6. If the procedure did not yield a unique choice, then it is necessary to examine the two-body purity. Repeat steps 3–5 taking advantage of Eq. (21). If this is not enough to yield a unique choice, then the procedure needs to be repeated for increasingly higher order purities until all available information has been exhausted or a unique choice has been determined. Note that coherences of higher order than the highest order purity available would not be able to be resolved. Section IV discusses representative examples of such a reconstruction.

IV. SOME EXAMPLES

We now illustrate the use of the reduced purities using the example of electronic decoherence in a molecular system due to electron-vibrational couplings. Specifically, we consider an oligoacetylene chain with 4 carbon atoms and 4 π electrons as described by the Su-Schrieffer-Heeger (SSH) Hamiltonian,[37] a tight-binding model with electron-vibrational interactions. The details of the Hamiltonian and the Ehrenfest mixed quantum-classical method employed to follow the vibronic dynamics have been specified before.[29,30,32] What is of relevance to this discussion is that the system consists of 4 non-interacting π electrons distributed among 4 spectrally isolated molecular orbitals $|\epsilon_n\rangle$ of energy ϵ_n that allow for double occupancy, for a total of 19 possible N-particle levels (without counting spin-degeneracies) subject to decoherence. The orbital energy and labels in the ground state optimal geometry of the chain are shown in Fig. 2. Computationally, we follow the dynamics of the one-body and two-body reduced density matrix for this system and use it to determine $P_1(t)$ and $P_2(t)$.

A. Decoherence of model superposition states

Consider first a "pure dephasing" example where there are no changes in the population of the Slater determinants during the dynamics. In this case, the decay of the reduced purities are directly indicative of decoherence. Specifically,
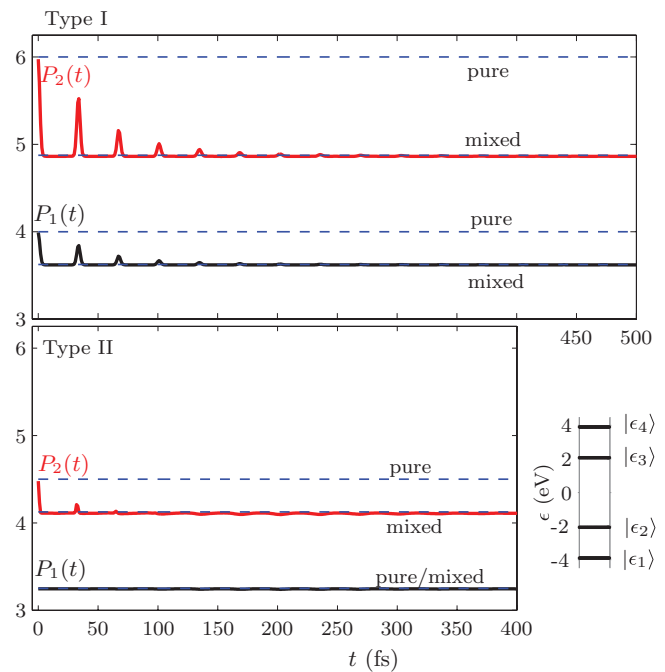

FIG. 2. Reduced purities during the vibronic evolution of a neutral oligoacetylene SSH chain with $N = 4$ electrons. The system is initially prepared in a superposition $|\Psi(0)\rangle = (c_0|\Phi_0\rangle + c_1|\Phi_1\rangle) \otimes |\chi_0\rangle$ ($|c_0|^2 = 3/4$ and $|c_1|^2 = 1/4$) between the ground state $|\Phi_0\rangle$ and an excited electronic state $|\Phi_1\rangle$. The initial nuclear state $|\chi_0\rangle$ is chosen to be the ground vibrational state associated with $|\Phi_0\rangle$. Type I: First order coherence, $|\Phi_1\rangle = \hat{c}_{\epsilon_3\uparrow}^\dagger \hat{c}_{\epsilon_2\uparrow} |\Phi_0\rangle$. Type II: Second order coherence, $|\Phi_1\rangle = \hat{c}_{\epsilon_3\downarrow}^\dagger \hat{c}_{\epsilon_2\downarrow} \hat{c}_{\epsilon_3\uparrow}^\dagger \hat{c}_{\epsilon_2\uparrow} |\Phi_0\rangle$. The dashed lines signal the fully coherent/incoherent limit of P_1 and P_2 computed using Eqs. (19) and (21) assuming that only $|\Phi_0\rangle$ and $|\Phi_1\rangle$ participate in the dynamics. The orbital labels and energies at initial time are shown in the bottom-right corner.

we follow the system-bath dynamics after preparation of the composite system in an initial separable superposition state of the form

$$|\Omega(0)\rangle = (c_0|\Phi_0\rangle + c_1|\Phi_1\rangle) \otimes |\chi_0\rangle, \qquad (22)$$

where $|\chi_0\rangle$ is the ground vibrational state in the ground electronic state $|\Phi_0\rangle$, and $|\Phi_1\rangle$ is an excited state. The $|\Phi_1\rangle$ is selected to be spectrally isolated from other N-particle states such that the vibronic evolution does not lead to population exchange into other levels, as revealed by constant orbital populations throughout the dynamics.

Two different types of initial superposition states are considered. In type I, $|\Phi_1\rangle = \hat{c}_{\epsilon_3\uparrow}^\dagger \hat{c}_{\epsilon_2\uparrow} |\Phi_0\rangle$ is obtained from the ground state via a HOMO→LUMO transition in a given spin channel, and the coherence order is 1. In type II, $|\Phi_1\rangle = \hat{c}_{\epsilon_3,\downarrow}^\dagger \hat{c}_{\epsilon_2,\downarrow} \hat{c}_{\epsilon_3,\uparrow}^\dagger \hat{c}_{\epsilon_2,\uparrow} |\Phi_0\rangle$ is a doubly excited state where the two electrons in the HOMO of $|\Phi_0\rangle$ are promoted into the LUMO, and the resulting coherence is of second order. Figure 2 shows the dynamics of the purities in these two cases for $|c_0|^2 = 3/4$ and $|c_1|^2 = 1/4$. The dashed lines in the figure indicate the fully coherent/incoherent behavior expected for P_1 and P_2 as computed from Eqs. (19) and (21) assuming that only $|\Phi_0\rangle$ and $|\Phi_1\rangle$ participate in the dynamics. In interpreting the results, it is useful to keep Fig. 1 in mind.

Focus first on the dynamics of the type I superposition (Fig. 2, top panel). At initial time, $P_1 = N$ and

$P_2 = N(N-1)/2$ because the system is pure and the coherence is of first order. The system-bath evolution leads to a decay of the purities that is entirely due to decoherence. Since $s_{10} = 1$, both P_1 and P_2 follow the coherence decay, and the fall of P_2 is $(N-1)$ times larger than the one of P_1. The partial recurrences in the purities signal vibronic evolution of the chain.[30] After 200 fs the system is well described as an incoherent mixture. In the type II case (Fig. 2, bottom panel), P_2 follows the decoherence while P_1 remains constant because it cannot distinguish a coherence of second order from a mixture of states. At initial time, P_2 takes its maximum value that is consistent with the superposition in question and evolves with the vibronic evolution. The dynamics of P_2 clearly shows decoherence in ~ 100 fs of a superposition of second order. Note that the observed decay of P_2 in this case is quantitatively smaller than the one observed in a first order coherence since the decoherence of lowest order has a larger impact in the two-body purity (recall Fig. 1).

B. Resonant photoexcitation

To illustrate the use of the reduced purities in a more complex setting, we now consider electronic decoherence due to vibronic interactions during resonant photoexcitation of a molecular system. This example illustrates how through an analysis of the reduced purities it is possible to establish the coherence properties of a N-particle system even when only the reduced density matrices are known. Contrary to the previous example, because of the photoexcitation, the populations of the involved Slater determinants change continuously during the dynamics.

Figure 3 shows the orbital energies, orbital populations, and reduced purities of the SSH chain during dipole-interaction with a continuous wave laser that is resonant with the HOMO-LUMO transition. Initially, the system is prepared in the ground vibronic state with an electronic state $|\Phi_0\rangle$ where the lowest energy molecular orbitals $|\epsilon_1\rangle$ and $|\epsilon_2\rangle$ are doubly occupied. As shown in Figs. 3(a) and 3(b), the laser promotes population into the $|\epsilon_3\rangle$ orbital. The reduced purities resulting from the numerical simulation are shown in black in Figs. 3(c) and 3(d). Because the laser induces changes in the state populations, simple inspection of P_1 and P_2 cannot reveal the nature of the coherences and an explicit model of the dynamics is required. From a N-particle perspective, the laser field can transfer population from $|\Phi_0\rangle$ into the degenerate pair

$$|\Phi_1\rangle = \hat{c}_{\epsilon_3\uparrow}\hat{c}_{\epsilon_2\uparrow}|G\rangle, \quad |\Phi_2\rangle = \hat{c}_{\epsilon_3\downarrow}\hat{c}_{\epsilon_2\downarrow}|G\rangle. \quad (23)$$

Supposing that only states $|\Phi_0\rangle$, $|\Phi_1\rangle$, and $|\Phi_2\rangle$ can participate in the dynamics, the N-particle density matrix of the system can be written as

$$\hat{\rho}_e = \sum_{n=0}^{2}\sum_{m=0}^{2} a_{nm}|\Phi_n\rangle\langle\Phi_m|. \quad (24)$$

We consider different models for $\hat{\rho}_e$ based on Eq. (24) that differ in the degree of assumed coherence and the states
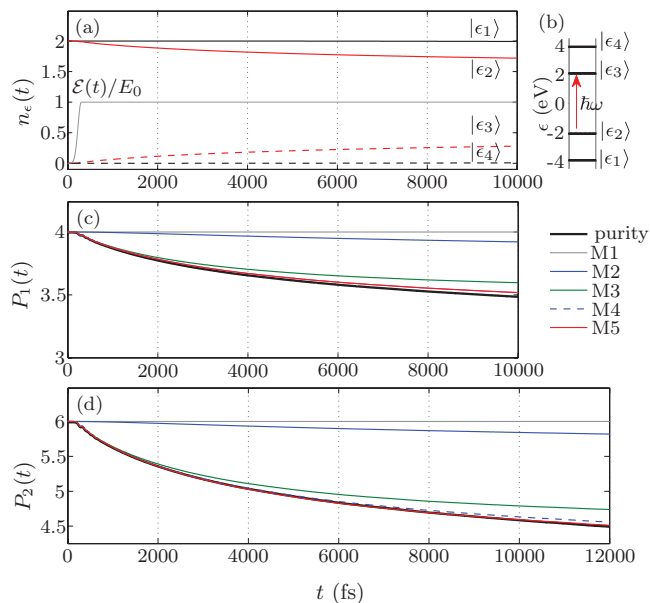

FIG. 3. Reduced purities during photoexcitation of a neutral SSH chain with 4 electrons. (a) Orbital populations during photoexcitation with a laser field $E(t) = \mathcal{E}(t)\cos(\omega t)$. The laser frequency $\hbar\omega = 4.08$ eV is chosen to be at resonance with the HOMO-LUMO transition. The envelope function $\mathcal{E}(t)$ has a Gaussian turn-on and remains constant at $E_0 = 8.7 \times 10^{-3}$ V/Å from $t = 300$ fs on. (b) Single-particle spectrum of the SSH chain at initial time. (c) One-body and (d) two-body purity during the dynamics. The black lines are the result of an explicit simulation of the vibronic dynamics. The colored lines correspond to different models with varying degrees of coherence assumed in the N-body density matrix (see text). In (c), the lines for **M3** and **M4** are on top of each other and cannot be distinguished.

involved. Specifically, we consider models

M1:	$|a_{nm}|^2 = a_{nn}a_{mm},$	$a_{22} = 0,$
M2:	$|a_{nm}|^2 = a_{nn}a_{mm},$	$a_{11} = a_{22},$
M3:	$a_{2n} = 0, \forall n,$	$a_{01} = 0,$
M4:	$a_{01} = a_{02} = 0,$	$a_{11} = a_{22},$
M5:	$a_{nm} = 0, \forall n \neq m,$	$a_{11} = a_{22}.$

These models correspond, respectively, to (**M1**) a coherent superposition between states $|\Phi_0\rangle$ and $|\Phi_1\rangle$ with no participation of $|\Phi_2\rangle$; (**M2**) a coherent superposition involving all three states; (**M3**) an incoherent mixture between states $|\Phi_0\rangle$ and $|\Phi_1\rangle$; (**M4**) a partially coherent triad where only the coherences between $|\Phi_1\rangle$ and $|\Phi_2\rangle$ are maintained; and (**M5**) a fully incoherent state. In the models where all three states are considered (M2, M4, and M5), we take $a_{11} = a_{22}$ since the $|\Phi_0\rangle \rightarrow |\Phi_1\rangle$ and $|\Phi_0\rangle \rightarrow |\Phi_2\rangle$ transition dipoles are identical. As shown below, only when the correct form for $\hat{\rho}_e$ is assumed the reduced purities reconstructed from Eqs. (19) and (21) match the reduced purity obtained directly from the numerical simulation.

In **M1**, $P_1 = N$ and $P_2 = N(N-1)/2$ (Fig. 3, grey lines) since two states involved are separated by a single-particle transition and are coherent (recall Eqs. (19) and (21)). This model fails to capture the observed decay of the purities as the photoexcitation proceeds and is not a faithful description of the system. The reduced purities for **M2** observe a decay (blue lines in Fig. 3) that is not due to decoherence but due to

the transfer of population into a pair of states $|\Phi_1\rangle$ and $|\Phi_2\rangle$ with $s_{12} = 2$. Nevertheless, the decay in the reduced purities in this model does not capture that observed in the simulation, indicating that a fully coherent model is not a faithful description of the system. In **M3**, the assumed decoherence between states $|\Phi_0\rangle$ and $|\Phi_1\rangle$ leads to a significant decrease in P_1 and P_2 (green lines, Fig. 3). However, the decay is not sufficient to explain the observed behavior indicating that a model where all 3 states are taken into account is required. Both three-state models **M4** (blue dashed lines) and **M5** (red lines) reproduce equally well the behavior of P_1. In fact, they are indistinguishable in P_1 since **M4** contains 2nd order coherences not present in the fully incoherent model **M5** that cannot be resolved by P_1. In order to determine which state represents best the state of the system, an analysis of P_2 is required. As shown in Fig. 3(d), the model that best adjusts to the observed behavior is **M5** indicating that during photoexcitation the system is best described as an incoherent mixture between states $|\Phi_0\rangle$, $|\Phi_1\rangle$, and $|\Phi_2\rangle$. This is because of the fast electronic decoherence timescale that is characteristic of the model and method employed.[30,32]

V. CONCLUSIONS

A family of reduced purity measures that can be used to characterize decoherence phenomena in many-electron systems has been introduced based on the hierarchy of electronic reduced density matrices. Using the properties of Slater determinants, explicit expressions for the one-body and two-body purities for a general electronic state have been derived and used to elucidate the structure and information content of the reduced purities. As shown, the reduced purities can be used to characterize electronic decoherence when only few-body electronic reduced density matrices are known. Further, the measures permit decomposing electronic decoherence phenomena into contributions arising from coherences of different order providing, in this way, a useful interpretative tool of the dynamics. The use of the reduced purities was exemplified via investigation of decoherence in a model molecular system with electron-vibrational interactions both in a pure dephasing case and in a case where the electronic structure is constantly changing due to resonant photoexcitation.

Subtleties can develop in the interpretation of the reduced purities because of the fact that we deal with a general many-electron subsystem but only use reduced information about the electronic degrees of freedom. In particular, a decay in the reduced purities is seen to arise either due to bath-induced decoherence or due to an increase in electronic correlation as both phenomena lead to nonidempotency of the reduced electronic density matrices. While it is technically clear how to define reduced purity measures that solely reflect decoherence properties via the Carlson-Keller theorem, these measures require knowledge of higher order electronic density matrices that are typically not available.

In the particular case of pure dephasing problems, the interpretation of the reduced purities is straightforward as a decay of the reduced purities directly signals coherence loss. For the more general case, a systematic procedure to determine the decoherence contributions to the reduced purities

was presented. Since such a procedure involves unraveling the observed dynamics of the few-body electronic density matrices into the N-particle Hilbert space, isolating a unique solution can only benefit from any additional information about the electronic subsystem that is available such as the active determinant space and the initial state.

At this point, it is useful to connect the proposed reduced purity measures with existing electronic structure, condensed matter, and quantum optics formalisms. From a time-dependent density functional perspective (TDDFT), in principle the reduced purities are functionals of the time-dependent density and the Kohn-Sham and many-body initial states[38–40] even for an open electronic subsystem. This functional dependence allows expressing the off-diagonals of all electronic reduced density matrices in terms of the diagonal elements of the reduced one-body density matrix in position representation. However, to date, this functional dependence is not fully known and cannot be exploited to further advance the present considerations. Other electronic structure theories that employ reduced density matrices, such as reduced density matrix functional theory (RDMFT),[41–43] currently focus on static problems of closed electronic systems. In these theories, the time-dependence and decoherence aspects of the reduced purities are expected to be of future relevance. Finally, similar purity measures are also applicable in quantum optics[44–46] and condensed matter physics[31,47] formalisms that employ the hierarchy of r-body Green's functions. This is because the r-body density matrices can be obtained from the equal-time limit of r-body Green's functions.

While this analysis has focused on purity related measures, the methods, insights, and limitations apply to any other measure of decoherence that is based on the density matrix such as the von Neumann entropy. Future prospects include studying the asymptotic thermal behavior of the reduced purities and the utility of these measures in characterizing increasingly more complex electron-bath dynamics.

[1]H. P. Breuer and F. Petruccione, *The Theory of Open Quantum Systems* (Oxford University Press, New York, 2002).

[2]M. Schlosshauer, *Decoherence and the Quantum-to-Classical Transition* (Springer, New York, 2008).

[3]E. Joos, H. D. Zeh, C. Kiefer, D. J. W. Giulini, J. Kupsch, and I. O. Stamatescu, *Decoherence and the Appearance of a Classical World in Quantum Theory*, 2nd ed. (Springer, 2003).

[4]W. H. Zurek, Phys. Today **44**(10), 36 (1991).

[5]B. G. Levine and T. J. Martínez, Annu. Rev. Phys. Chem. **58**, 613 (2007).

[6]Y.-C. Cheng and G. R. Fleming, Annu. Rev. Phys. Chem. **60**, 241 (2009).

[7]F. Ortmann, F. Bechstedt, and K. Hannewald, Phys. Rev. B **79**, 235206 (2009).

[8]S. H. Choi, C. Risko, M. C. R. Delgado, B. Kim, J.-L. Brédas, and C. D. Frisbie, J. Am. Chem. Soc. **132**, 4358 (2010).

[9]G. S. Engel, T. R. Calhoun, E. L. Read, T.-K. Ahn, T. Mancal, Y.-C. Cheng, R. E. Blankenship, and G. R. Fleming, Nature (London) **446**, 782 (2007).

[10]E. Collini, C. Y. Wong, K. E. Wilk, P. M. G. Curmi, P. Brumer, and G. D. Scholes, Nature (London) **463**, 644 (2010).

[11]P. Brumer and M. Shapiro, Proc. Natl. Acad. Sci. U.S.A. **109**, 19575 (2012).

[12]L. A. Pachon and P. Brumer, Phys. Chem. Chem. Phys. **14**, 10094 (2012).

[13]L. A. Pachón and P. Brumer, Phys. Rev. A **87**, 022106 (2013).

[14]R. Kapral, Annu. Rev. Phys. Chem. **57**, 129 (2006).

[15]U. Weiss, *Quantum Dissipative Systems*, 2nd ed. (World Scientific, Singapore, 1999).

[16]T. Winzer, A. Knorr, and E. Malic, Nano Lett. **10**, 4839 (2010).

[17]E. Malic, T. Winzer, E. Bobkin, and A. Knorr, Phys. Rev. B **84**, 205406 (2011).

[18]J. Yuen-Zhou, C. Rodríguez-Rosario, and A. Aspuru-Guzik, Phys. Chem. Chem. Phys. **11**, 4509 (2009).

[19]J. Yuen-Zhou, D. G. Tempel, C. A. Rodríguez-Rosario, and A. Aspuru-Guzik, Phys. Rev. Lett. **104**, 043001 (2010).

[20]H. Appel and M. Di Ventra, Phys. Rev. B **80**, 212303 (2009).

[21]H. Appel and M. D. Ventra, Chem. Phys. **391**, 27 (2011).

[22]M. Shapiro and P. Brumer, *Quantum Control of Molecular Processes* (Wiley-VCH, Weinheim, 2012).

[23]S. A. Rice and M. Zhao, *Optical Control of Molecular Dynamics* (John Wiley & Sons, New York, 2000).

[24]M. Nielsen and I. Chuang, *Quantum Computation and Quantum Information* (Cambridge University Press, 2000).

[25]L. Cohen and C. Frishberg, Phys. Rev. A **13**, 927 (1976).

[26]M. Bonitz, *Quantum Kinetic Theory* (Teubner, Stuttgart, 1998).

[27]B. J. Schwartz, E. R. Bittner, O. V. Prezhdo, and P. J. Rossky, J. Chem. Phys. **104**, 5942 (1996).

[28]H. Hwang and P. J. Rossky, J. Phys. Chem. B **108**, 6723 (2004).

[29]I. Franco, M. Shapiro, and P. Brumer, J. Chem. Phys. **128**, 244905 (2008).

[30]I. Franco and P. Brumer, J. Chem. Phys. **136**, 144501 (2012).

[31]A. L. Fetter and J. D. Walecka, *Quantum Theory of Many-Particle Systems* (Dover Publications, Mineola, NY, 2003).

[32]I. Franco, A. Rubio, and P. Brumer, New J. Phys. **15**, 043004 (2013).

[33]T. D. Crawford and H. F. Schaefer, in *Reviews in Computational Chemistry*, edited by K. B. Lipkowitz and D. B. Boyd (John Wiley & Sons, 2007), pp. 33–136.

[34]P. Ziesche, Int. J. Quantum Chem. **56**, 363 (1995).

[35]P. Gersdorf, W. John, J. P. Perdew, and P. Ziesche, Int. J. Quantum Chem. **61**, 935 (1997).

[36]B. C. Carlson and J. M. Keller, Phys. Rev. **121**, 659 (1961).

[37]A. J. Heeger, S. Kivelson, J. R. Schrieffer, and W. P. Su, Rev. Mod. Phys. **60**, 781 (1988).

[38]E. Runge and E. K. U. Gross, Phys. Rev. Lett. **52**, 997 (1984).

[39]T. Kreibich and E. K. U. Gross, Phys. Rev. Lett. **86**, 2984 (2001).

[40]*Fundamentals of Time-Dependent Density Functional Theory*, Lecture Notes in Physics Vol. 837, edited by M. A. L. Marques, N. T. Maitra, F. Nogueira, E. K. U. Gross, and A. Rubio (Springer, Berlin, 2012).

[41]A. J. Coleman, Rev. Mod. Phys. **35**, 668 (1963).

[42]T. L. Gilbert, Phys. Rev. B **12**, 2111 (1975).

[43]O. Gritsenko, K. Pernal, and E. J. Baerends, J. Chem. Phys. **122**, 204102 (2005).

[44]L. Mandel and E. Wolf, *Optical Coherence and Quantum Optics* (Cambridge University Press, Melbourne, 1995).

[45]M. O. Scully and M. S. Zubairy, *Quantum Optics* (Cambridge University Press, 1997).

[46]R. Loudon, *The Quantum Theory of Light*, 3rd ed. (Oxford University Press, 2000).

[47]P. C. Martin and J. Schwinger, Phys. Rev. **115**, 1342 (1959).